MATHEMATICAL ENGINEERING
TECHNICAL REPORTS

Computer-Aided Creation of Impossible Objects and Impossible Motions

Kokichi Sugihara

METR 2007–41 July 2007

DEPARTMENT OF MATHEMATICAL INFORMATICS
GRADUATE SCHOOL OF INFORMATION SCIENCE AND TECHNOLOGY
THE UNIVERSITY OF TOKYO
BUNKYO-KU, TOKYO 113-8656, JAPAN

WWW page: http://www.i.u-tokyo.ac.jp/mi/mi-e.htm

Computer-Aided Creation of Impossible Objects and Impossible Motions

Kokichi Sugihara
University of Tokyo

July 9, 2007

Abstract

There is a class of pictures called "pictures of impossible objects". These pictures generate optical illusion; when we see them, we have impression of solid objects and at the same time we feel that such solids cannot be realized. Although they are called "impossible", they are not necessarily impossible; some of them can be realized as real solids. This is because a single picture does not convey enough information about depth. Using the same trick, we can also design what may be called "impossible motions". That is, we can construct a shape of a solid which looks like an ordinary solid but which admits physical motions that look like impossible. A computer-aided method for creating impossible objects and impossible motions is presented with examples.

1 Introduction

Optical illusion is one of the most interesting research topics in visual psychology, and has been studied extensively [10, 14]. However, there are a number of different types of optical illusion and unified study seems difficult; each type of optical illusion is studied individually. Among them, a class of pictures called "pictures of impossible objects" forms a special type of illusion in that it is related to three-dimensional structures while other optical illusions are primarily related to two-dimensional structures.

The pictures of impossible objects are the pictures which, when we see them, give us some ideas of three-dimensional object structures but at the same time give us the impression that they cannot be realized in the three-dimensional space. A typical old example of the impossible objects is the Penrose triangle [13] found in 1958.

In addition to the area of visual psychology, the impossible objects have also been studied from a mathematical point of view. One of the pioneers is Huffman, who characterized impossible objects from a viewpoint of computer interpretation of line drawings [11]. Clowes [2] also proposed a similar

idea in a different manner. Cowan [3, 4] and Térouanne [20] characterized a class of impossible objects that are topologically equivalent to a torus. Draper studied pictures of impossible object through the gradient space [6]. Sugihara classified pictures of impossible objects according to his algorithm for interpretation of line drawings [15, 17].

Artists also use impossible objects as material for artistic work. One of the most famous examples is the endless loop of stairs drawn by Dutch artist M. C. Escher in his work titled "Klimmen en dalen (Ascending and descending)" [8]. Other examples include painting by Mitsumasa Anno [1] and drawings by Sandro del Prete [7], to mention a few.

While those activities are stories about two-dimensional pictures, several tricks have also been found for realization of impossible objects as actual three-dimensional structures. The first trick is to use curved surfaces for faces that look planar; Mathieu Hamaekers generated the Penrose triangle by this trick [7]. The second trick is to generate hidden gaps in depth; Shigeo Fukuda used this trick and generated a solid model of Escher's "Waterfall" [7].

This paper shows that some "impossible" objects can be realized as three-dimensional solids even if those tricks are not employed; in other words, "impossible" objects can be realized under the conditions that faces are made by planar (non-curved) polygons and that object parts are actually connected whenever they look connected in the picture plane. For example, Figure 1(a) shows a line drawing representing a V-shape solid with a horizontal bar. Exchanging the visible parts and hidden parts, we get the line drawing in (b), which belongs to the class of pictures of impossible objects. However, this impossible object can be realized as a solid in the three-dimensional space as shown in Figure 1(c).

Such solid models can generate visual illusions in the sense that although we are looking at actual objects, we feel that those objects can not exist.

The same trick can also be used to generate a new class of visual illusion called "impossible" physical motions. The basic idea is as follows. Instead of pictures of impossible objects, we choose pictures of ordinary objects around us, and reconstruct solid models from these pictures using the non-rectangularity trick. The resulting solid models are unusual in their shapes although they look ordinary. Because of this gap between the perceived shape and the actual shape, we can add actual physical motions that look like impossible.

The organization of the paper is as follows. In Section 2, we review the basic method for judging the realizability of a solid from a given picture, and in Section 3, we review the robust method for reconstructing objects from pictures. In Section 4, we study algorithmic aspect of our robust method. We show examples of the three dimensional realization of impossible objects and impossible motions in Section 5, and give conclusions in Section 6.

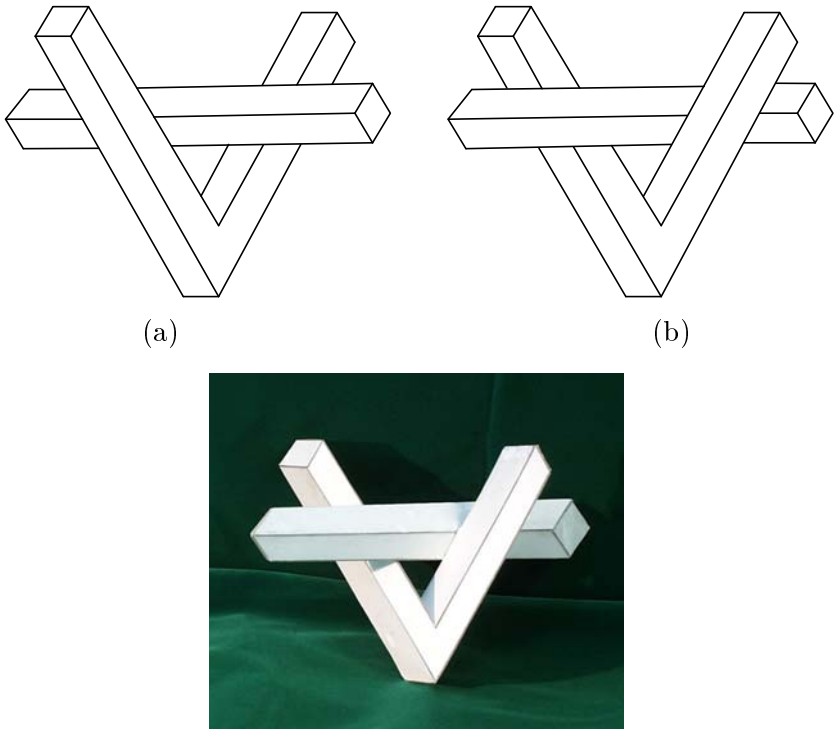

(a) (b)

(c)

Figure 1. Three-dimensional realization of impossible V and bar: (a) ordinary picture; (b) picture of an impossible object; (c) solid model realizing the picture in (b).

2 Ambiguity in Depths

In this section we briefly review the algebraic structure of the freedom in the choice of the polyhedron represented by a picture [17]. This gives the basic tool with which we construct our algorithm for designing impossible motions.

As shown in Figure 2, suppose that an (x, y, z) Cartesian coordinate system is fixed in the three-dimensional space, and a given polyhedral object P is projected by the central projection with respect to the center at the origin $\mathrm{O} = (0, 0, 0)$ onto the picture plane $z = 1$. Let the resulting picture be denoted by D. If the polyhedron P is given, the associated picture D is uniquely determined. On the other hand, if the picture D is given, the associated polyhedron is not unique; there is large freedom in the choice of the polyhedron whose projection coincides with D. The algebraic structure of the degree of freedom can be formulated in the following way.

For a given polyhedron P, let m be the number of vertices, $V = \{v_1, v_2, \ldots, v_m\}$ be the set of all the vertices of P, n be the number of faces, $F = \{f_1, f_2, \ldots, f_n\}$

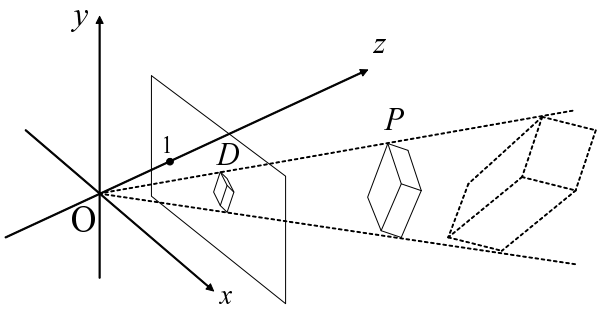

Figure 2. Different solids can generate the same picture.

be the set of all the faces of P, and R be the set of all pairs (v_i, f_j) of vertices v_i $(\in V)$ and faces f_j $(\in F)$ such that v_i is on f_j. We call the triple $I = (V, F, R)$ the *incidence structure* of P.

Let (x_i, y_i, z_i) be the coordinates of the vertex v_i $(\in V)$, and let

$$a_j x + b_j y + c_j z + 1 = 0 \tag{1}$$

be the equation of the plane containing the face f_j $(\in F)$. The central projection $v_i' = (x_i', y_i', z_i')$ of the vertex v_i onto the picture plane $z = 1$ is given by

$$x_i' = x_i/z_i, \quad y_i' = y_i/z_i, \quad z_i' = 1. \tag{2}$$

Suppose that we are given the picture D and the incidence structure $I = (V, F, R)$, but we do not know the exact shape of P. Then, the coordinates of the projected vertices x_i' and y_i' are given constants, while z_i $(i = 1, 2, \ldots, m)$ and a_j, b_j, c_j $(j = 1, 2, \ldots, n)$ are unknown variables. Let us define

$$t_i = 1/z_i, \tag{3}$$

and treat t_i as unknown variable instead of z_i. Then, we get from (2)

$$x_i = x_i'/t_i, \quad y_i = y_i'/t_i, \quad z_i = 1/t_i. \tag{4}$$

Assume that $(v_i, f_j) \in R$. Then, the vertex v_i is on the face f_j, and hence

$$a_j x_i + b_j y_i + c_j z_i + 1 = 0 \tag{5}$$

should be satisfied. Substituting (4), we get

$$x_i' a_j + y_i' b_j + c_j + t_i = 0, \tag{6}$$

which is linear in the unknowns a_j, b_j, c_j and t_i because x_i' and y_i' are known constants.

Collecting the equations of the form (6) for all $(v_i, f_j) \in R$, we get the system of linear equations, which we denote by

$$A\boldsymbol{w} = 0, \tag{7}$$

where $\boldsymbol{w} = (t_1, \ldots, t_m, a_1, b_1, c_1, \ldots, a_n, b_n, c_n)$ is the vector of unknown variables and A is a constant matrix.

The picture D also gives us information about the relative depth between a vertex and a face. Suppose that a visible face f_j hides a vertex v_i. Then, f_j is nearer to the origin than v_i, and hence we get

$$x_i' a_j + y_i' b_j + c_j + t_i < 0. \tag{8}$$

If the vector v_i is nearer than the face f_j, then we get

$$x_i' a_j + y_i' b_j + c_j + t_i > 0. \tag{9}$$

Collecting all of such inequalities, we get a system of linear inequalities, which we denote by

$$B\boldsymbol{w} > 0, \tag{10}$$

where B is a constant matrix.

The linear constraints (7) and (10) specify the set of all possible polyhedron represented by the given picture D. In other words, the set of all $\boldsymbol{w}$'s that satisfy the equations (7) and the inequalities (10) represents the set of all possible polyhedrons represented by D. Actually the next property holds [17].

Property 1 (correctness of a picture). Picture D represents a polyhedron if and only if the system of linear equations (7) and inequalities (10) has a solution. ∎

Hence, to reconstruct a polyhedron from a given picture D is equivalent to choose a vector $\boldsymbol{w}$ that satisfies (7) and (10). (Refer to [17] for the formal procedure for collecting the equation (7) and the inequalities (10) and for the proof of this property.)

3 Removal of Superstrictness

As seen in the last section, we can characterize the set of all polyhedra represented by a given picture in terms of linear constraints. However, these constraints are too strict if we want to apply them to actual reconstruction procedure. This can be understood by the next example.

Consider the picture shown in Figure 3(a). We, human beings, can easily interpret this picture as a truncated pyramid seen from above. However, if we search by a computer for the vectors w that satisfy the constraints (7) and (10), the computer usually judges that the constraints (7) and (10) are

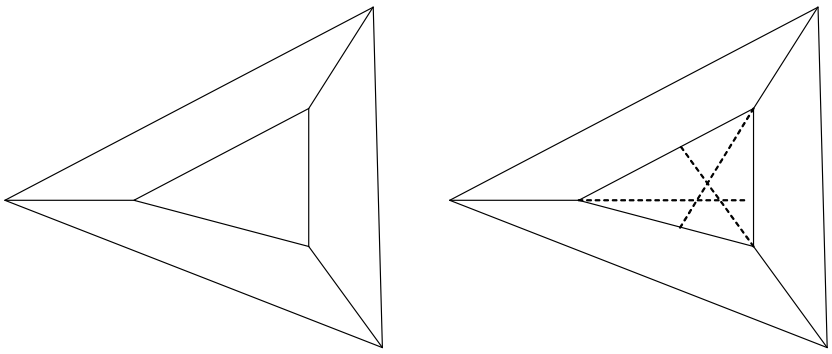

(a) (b)

Figure 3. Picture of a truncated pyramid: (a) a picture which we can easily interpret as a truncated pyramid; (b) incorrectness of the picture due to lack of the common point of intersection of the three side edges that should be the apex of the pyramid.

not satisfiable and hence the picture in Figure 3(a) does not represent any polyhedron.

This judgment is mathematically correct because of the following reason.

Suppose that Figure 3(a) represents a truncated pyramid seen from above. Then, the three side faces should have a common point of intersection when they are extended. Since this point is also on the common edge of two side faces, it should also be the common point of intersection of the three side edges of the truncated pyramid. However, as shown by the broken lines in Figure 3(b), the three edges are not concurrent. Therefore, this picture is not a projection of any truncated pyramid. The object can be reconstructed only when we use curved faces instead of planar faces.

By this example, we can understand that the satisfiability of the constraints (7) and (10) does not give a practical solution of the problem of recognizing the reconstructability of polyhedra from a picture. Indeed, numerical errors cannot be avoided when the pictures are represented in a computer, and hence the picture of a truncated pyramid becomes almost always incorrect even if one carefully draws it in such a way that the three edges meet at a common point.

This superstrictness of the constraints comes from redundancy of the equations. When the vertices of the truncated pyramid were placed at strictly correct positions in the picture plane, the associated coefficient matrix A is not of full rank. When those vertices contain digitization errors, the rank of A increases and consequently the set of constraints (7) and (10) becomes inconsistent.

To make a practical method for judging the reconstructability of polyhedra, we should remove redundant equations from (10). For this purpose, the

next property is helpful. Assume that a picture with the incidence structure $I = (V, F, R)$ is given. For subset $X \subset F$, let us define

$$V(X) \equiv \{v \in V \mid (\{v\} \times X) \cap R \neq \emptyset\}, \tag{11}$$

$$R(X) \equiv (V \times X) \cap R, \tag{12}$$

that is, $V(X)$ $(\subset V)$ denotes the set of vertices that are on at least one face in X, and $R(X)$ $(\subset R)$ denotes the set of incidence pairs (v, f) such that $f \in X$. For any finite set X, let $|X|$ denote the number of elements in X. Then the next property holds [17].

Property 2 (nonredundancy of equations). The associated set of equations (10) is nonredundant if and only if

$$|V(X)| + 3|X| \geq |R(X)| + 4 \tag{13}$$

for any subset $X \subset F$ such that $|X| \geq 2$. ∎

Refer to [Sugihara 1986] for the strict meaning of "nonredundant" and for the proof.

Let us see how this property works by an example. The picture in Figure 3(a) has 6 vertices and five faces (including the rear face) and hence $|V| + 3|F| = 21$. On the other hand, this picture has 2 triangular faces and 3 quadrilateral faces, and hence has $|R| = 2 \times 3 + 3 \times 4 = 18$ incidence pairs in total. Therefore, the inequality (13) is not satisfied and consequently we can judge that the associated equations are redundant. Property 2 also tells us that if we remove any one equation from (10), the resulting equation becomes nonredundant.

In this way, we can use this property to judge whether the given incidence structure generates redundant equations, and also to remove redundancy if redundant.

Using Properties 1 and 2, we can design a robust method for reconstructing a polyhedron from a given picture in the following way.

Suppose that we are given a picture. We first construct the equations (7) and the inequalities (10). Next, using Property 2, we judge whether (7) is redundant, and if redundant, we remove equations one by one until they become nonredundant. Let the resulting equations be denoted by

$$A'w = 0, \tag{14}$$

where A' is a submatrix of A obtained by removing the rows corresponding to redundant equations. Finally, we judge whether the system of (10) and (14) has solutions. If it has, we can reconstruct the solid model corresponding to an arbitrary one of the solutions. If it does not, we judge that the picture does not represent any polyhedron.

With the help of this procedure, Sugihara found that actual solid models can be reconstructed from some of pictures of impossible objects [18, 19].

4 Efficient Recognition of Superstrictness

The next problem is how to check the condition in Property 2 efficiently. There are $O(2^n)$ subsets of F, and hence if we check the inequality (13) for each subset one by one, it would take an exponential time. We have to construct an efficient method in order to use the property for practical use. To this goal, we change the inequality in the following way. Suppose that we are given an incidence structure $I = (V, F, R)$. For subset $Y \subset R$, let us define

$$V(Y) = \{v \in V \mid (\{v\} \times F) \cap Y \neq \emptyset\}, \tag{15}$$

$$F(Y) = \{f \in F \mid (V \times \{f\}) \cap Y \neq \emptyset\}. \tag{16}$$

That is, $V(Y)$ is the set of vertices included in at least one equation in Y, and $F(Y)$ is the set of faces included in at least one equation in Y.

Then, the next property holds [17].

Property 3. For an incidence structure $I = (V, F, R)$, the following (i) and (ii) are equivalent.

(i) the inequality (13) is satisfied for any $X \subset F$ such that $|X| \geq 2$.
(ii) the inequality

$$|Y| + 4 \leq |V(Y)| + 3|F(Y)| \tag{17}$$

is satisfied for any $Y \subset R$ such that $|F(Y)| \geq 2$. ∎

Refer to Sugihara [17] for the proof of this property.

Let us consider intuitive meaning of the inequality (17). The first term of the left-hand side of (17) represents the number of equations in Y, and the second term represents the minimum degree of freedom for us to reconstruct a solid object from its projection. Recall that we have to give the z values of three vertices to fix the plane passing them, and have to give at least one more z value of a vertex to specify the thickness of the solid.

On the other hand, the right-hand side of (17) represents the number of unknowns included in Y, because each vertex has one unknown and each face has three unknowns.

Therefore, the inequality (17) says that for any subset Y of equations related to two or more faces, Y should contain at least $|Y| + 4$ unknowns. This is a general condition for a system of equations with nonzero degrees of freedom to be structurally consistent.

Let $G = (R, V \cup F, W)$ be the bipartite graph having the left node set R and the right node set $V \cup F$ and the arc set $W \subset R \times (V \cup F)$ such that $(r, v), (r, f) \in W$ if and only if the equation $r \in R$ represents that the vertex v should be on the face f. From G we construct network N in the following way. As shown in Figure 4, we add source node s and sink node t in such a way that s is connected to all nodes in R by directed arcs with capacity 1, all nodes in V are connected to t by directed arcs with capacity 1, and

all nodes in F are connected to t by arcs with capacity 3. Furthermore, we regard the arcs of G as directed arcs from R to $V \cup F$ with capacity ∞. We consider flow from s to t along arcs such that the amount of flow coming in is equal to that going out at every node in $R \cup V \cup F$ and the amount of flow along an edge does not exceed the associated capacity.

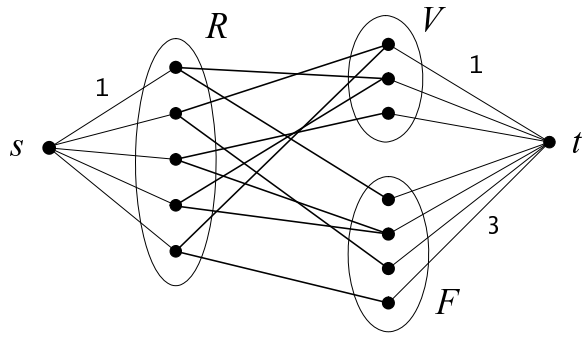

Figure 4. Network associated with the incidence structure $I = (V, F, R)$.

Then, the next property in well known [9, 12].

Property 4. The maximum flow from s to t in the network N coincides with $|R|$ if and only if

$$|X| \leq |V(X)| + 3|F(X)| \tag{18}$$

is satisfied for any $X \subset R$. ∎

Using maximum flow algorithms, we can construct the maximum flow of N efficiently, and hence can check the inequality (18) for all $X \subset R$ efficiently.

Note that our inequality (17) is similar to (18); the only difference is the term "4" in the left-hand side. In order to check the inequality (17), we modify the network N by adding one left node q and arc (s, q) with capacity 4, as shown in Figure 5. Next, we add two arcs from q, one to F and the other to $V \cup F$, as shown by broken lines in Figure 5. For every possible connection we construct the maximum flow and see if its value is equal to $|R| + 4$, and thus check the condition (ii) stated in Property 3 efficiently. Actually we can check it in $O(n^2)$ time by some additional tricks. Refer to [16] for details.

Thus, we can check the superstrictness of the picture, and remove redundant equations from (17) efficiently. Combining this with Property 1, we can check the correctness of line drawings efficiently, and consequently can find realizable impossible objects.

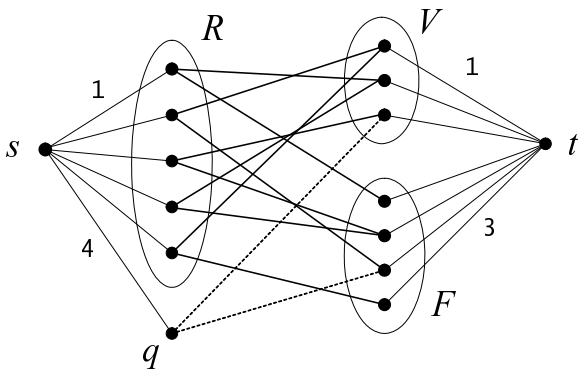

Figure 5. Augmented network for checking the superstructures of a picture.

5 Examples

The first examples of the realization of the impossible object shown in Figure 1(c) was constructed in the following manner. First, we constructed the system of equations (7) for the picture in Figure 1(b), then, removed redundant equations using Theorem 2 and got a non-redundant system (14) of equations. Next, we got a solution of eq. (14), which represents a specific shape of the three-dimensional solid. Finally, we computed the figure of the unfolded surface of this solid, and made a paper model by hands.

Figure 6 shows another view of this solid. As we can understand from this figure, the faces are not rectangular.

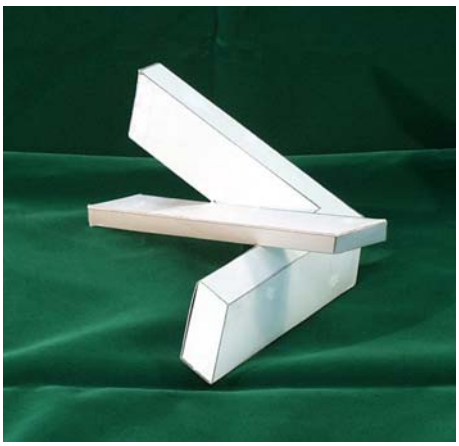

Figure 6. The same object as shown in Figure 1(c) seen from a different viewpoint.

Figure 7(a) shows another example of an impossible object constructed in a similar manner. In this object, the near-far relations of the poles seem inconsistent; the left pole is nearer than the other on the floor while it is

farther at the ceiling. This inconsistent structure is essentially similar to that represented by Escher's lithograph "Belvédère" in 1958. Figure 5(b) shows the same solid seen from a different direction.

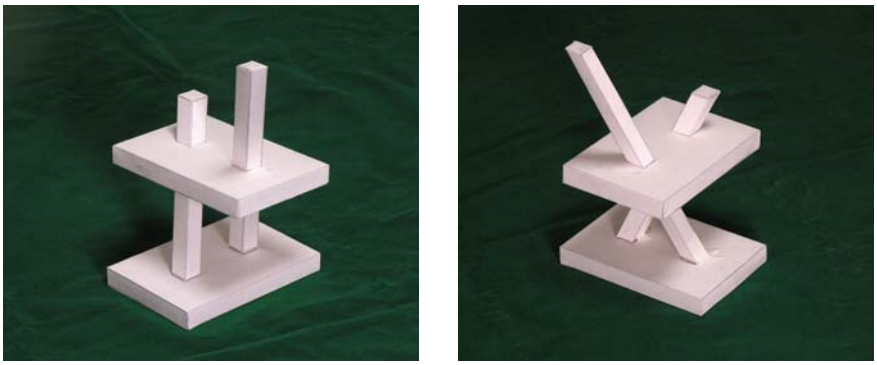

(a) (b)

Figure 7. "Impossible" columns: (a) shows an impossible structure which is similar to Escher's lithograph "Belvédère"; (b) shows another view of the same solid.

Next, let us consider "impossible" physical motions. A typical example of impossible motions is represented in Escher's lithograph "Waterval" in 1961, in which water is running uphill through the water path and is falling down at the waterfall, and is running uphill again. This motion is really impossible because otherwise an eternal engine could be obtained but that contradicts the physical law.

However, this impossible motion is realizable partially in the sense that material looks running uphill a slope. An example of this impossible motion is shown in Figure 8. Figure 8(a) shows a solid consisting of three slopes, all of which go down from the right to the left. If we put a ball on the left edge of the leftmost slope, as shown in Figure 8(a), the ball moves climbing up the slope from the left to the right; thus the ball admits an impossible motion.

The actual shape of this solid can be understood if we see Figure 8(b), which is the photograph of the same solid as in Figure 8(a) seen from another direction. From this figure, we can see that actually the ball is just rolling down the slope according to the natural properties of the ball and the slope.

Still another example is shown in Figure 9. In this figure, there are two walls with windows, but a straight bar passes through them in an unusual way.

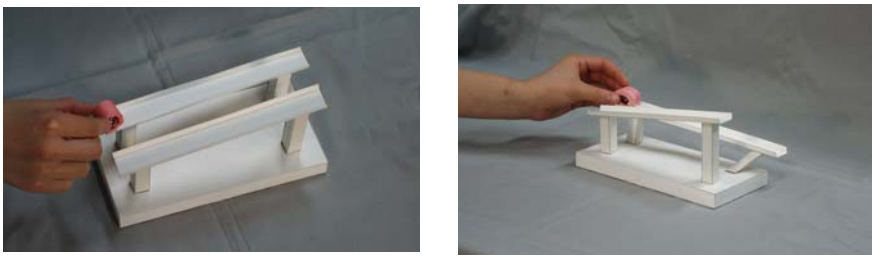

(a) (b)

Figure 8. Impossible motion of a ball along "Antigravity Parallel Slopes": (a) a ball climbing up a slope; (b) another view of the same situation.

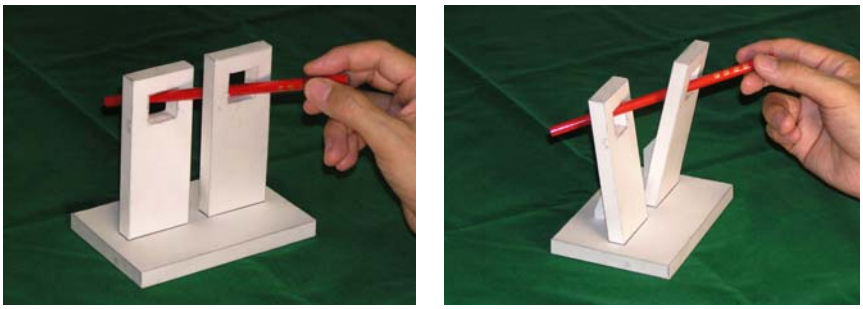

(a) (b)

Figure 9. "Soft Walls": (a) a straight bar passing throw the two windows in an unusual manner; (b) another view.

6 Concluding Remarks

We have presented a computer-aided method for creating "impossible" objects and "impossible" motions. We formulated the design of a solid admitting impossible objects and motions as a search for feasible solutions of a system of linear equations and inequalities. The resulting method enables us to realize impossible objects in the three-dimensional space.

The impossible objects and motions obtained by this method can offer a new type of optical illusion. When we see these objects and motions, we have a strange impression; we feel they are impossible although we are looking at them. One of our future works is to study this type of optical illusion from a view point of visual psychology.

Other problems for future include (1) to collect other variations of impossible objects and impossible motors, (2) to find criteria for choosing the best shape of an impossible solid among infinitely many possible shapes, and (3) to apply impossible objects to space art such as sculptures and buildings.

References

[1] M. Anno, *Book of ABC* (in Japanese), Fukuinkan-Shoten, Tokyo, 1974.

[2] M. B. Clowes, "On seeing things," *Artificial Intelligence*, vol. 2, pp. 79–116, 1971.

[3] T. M. Cowan, "The theory of braids and the analysis of impossible figures," *Journal of Mathematical Psychology*, vol. 11, pp. 190–212, 1974.

[4] T. M. Cowan, "Organizing the properties of impossible figures," *Perception*, vol. 6, pp. 41–56, 1977.

[5] H. S. M. Coxeter, M. Emmer, R. Penrose and M. L. Teuber, *M. C. Escher — Art and Science*, North-Holland, Amsterdam, 1986.

[6] S. W. Draper, "The Penrose triangle and a family of related figures," *Perception*, vol. 7, pp. 283–296, 1978.

[7] B. Ernst, *The Eye Beguiled*, Benedict Taschen Verlag GmbH, Köln, 1992.

[8] M. C. Escher, *Evergreen*, Benedict Taschen Verlag GmbH, Köln", 1993.

[9] L. R. Ford, Jr., and D. R. Fulkerson, *Flows in Network*, Princeton University Press, Princeton, New Jersey, 1962.

[10] R. L. Gregory, *The Intelligent Eye*, third edition, Weiderfeld and Nicolson, London, 1971.

[11] D. A. Huffman, "Impossible objects as nonsense sentences," In *Machine Entelligence*, B. Metzer and D. Michie (eds.), vol. 6, Edinburgh University Press, 1971.

[12] M. Iri, *Network Flow Transportation and Scheduling: Theory and Algorithms*, Academic Press, New York, 1969.

[13] L. S. Penrose and R. Penrose, "Impossible objects — A special type of visual illusion," *British Journal of Psychology*, vol. 49, pp. 31–33, 1958.

[14] J. O. Robinson, *The Psychology of Visual Illusion*, Hutchinson, London, 1972.

[15] K. Sugihara, "Classification of impossible objects," *Perception*, vol. 11, pp. 65–74, 1982.

[16] K. Sugihara, "Detection of structural inconsistency in systems of equations with degrees of freedom and its applications," *Discrete Applied Mathematics*, vol. 10, pp. 297–312, 1985.

[17] K. Sugihara, *Machine Interpretation of Line Drawings*, MIT Press, Cambridge, 1986.

[18] K. Sugihara, *Joy of Impossible Objects* (in Japanese), Iwanami-Shoten, Tokyo, 1997.

[19] K. Sugihara, "Three-dimensional realization of anomalous pictures—An application of picture interpretation theory to toy design," *Pattern Recognition*, vol. 30, no. 9, pp. 1061–1067, 1997.

[20] E. Térouanne, "On a class of 'Impossible' figures: A new language for a new analysis," *Journal of Mathematical Psychology*, vol. 22, pp. 20–47, 1980.